Topological Nernst effect in a three-dimensional skyrmion-lattice phase

Y. Shiomi,[1,*] N. Kanazawa,[1] K. Shibata,[1] Y. Onose,[2] and Y. Tokura[1,3]

[1]*Department of Applied Physics and Quantum Phase Electronics Center (QPEC), University of Tokyo, Tokyo 113-8656, Japan*

[2]*Department of Basic Science, University of Tokyo, Tokyo 153-8902, Japan*

[3]*RIKEN Center for Emergent Matter Science (CEMS), Wako 351-0198, Japan*

(Received 29 April 2013; revised manuscript received 31 July 2013; published 12 August 2013)

By measuring electrical Hall, thermal Hall, and Nernst effects, we have comprehensively investigated the topological transport properties associated with the Berry phase of noncoplanar spin structure in a possible skyrmion-lattice phase of MnGe. While the topological terms in thermal and electrical Hall conductivity decrease rapidly with temperature elevation, that in the Nernst effect can be discerned up to near the magnetic transition temperature. The topological term in transverse Peltier conductivity obeys the Mott relation and changes with temperature in proportion to the three-dimensional density of the topological spin texture. This result indicates that three dimensionally ordered skyrmions are responsible for the topological transport phenomena in MnGe.

DOI: 10.1103/PhysRevB.88.064409 PACS number(s): 72.15.Eb, 72.15.Jf, 72.25.Ba

I. INTRODUCTION

Skyrmions, the concept of which was first introduced in the field of nuclear physics by Skyrme,[1] have recently been discovered to be the physical identity in solids. Neutron diffraction[2–7] and Lorentz transmission electron microscopy[8–10] measurements have revealed spin swirling objects which form a triangular lattice in chiral helimagnets, e.g., MnSi,[2–4] $Mn_{1-x}Fe_xSi$,[3] $Fe_{1-x}Co_xSi$,[3,5,8] FeGe,[6,9] and Cu_2OSeO_3.[7,10] One unit of the magnetic texture corresponds to the skyrmion with the topological charge of -1. The skyrmion, in which the constituent spins subtend the solid angle of 4π, hosts the scalar spin chirality, which endows the conduction electrons with the Berry phase and gives rise to emergent electromagnetic phenomena, such as the topological Hall effect (THE)[11–14] and electromotive force induced by skyrmion motion.[15] In the THE, the scalar spin chirality defined on localized three-spins, $\boldsymbol{S}_i \cdot (\boldsymbol{S}_j \times \boldsymbol{S}_k)$, acts like a fictitious flux and leads to the Hall response. The signal of the THE has been observed in the skyrmion-lattice phase of MnSi (Refs. 11–13) and of FeGe.[14] In these materials, the THE is caused by the real-space Berry phase, which is proportional to the real-space skyrmion density.[16] When a large electric current above a threshold value is applied, skyrmions begin to move and the resultant temporal variation of the fictitious flux causes the emergent electromotive force along the Hall direction.[15] In analogy to these intriguing charge-transport features of the skyrmion lattice, the topological thermal or thermoelectric transport properties are also of great interest, although seldom investigated. The skyrmion phase is usually limited in a very narrow temperature (T) range (<1 K) for the aforementioned materials, which has made it difficult to experimentally study the thermal and thermoelectric transport phenomena.

Recently found MnGe is a suitable candidate material to overcome this difficulty, because a possible skyrmion-lattice ground state emerges over wide T and the magnetic-field (H) region and also because the large THE, which is a characteristic event in a noncoplanar magnetic order, has been observed there.[17,18] MnGe, which can be prepared only by high-pressure synthesis, has a $B20$-type chiral crystal lattice, isostructural with MnSi.[17] MnGe shows the magnetic transition to a multiple-q state at $T_N \approx 170$ K, which has been assigned to the skyrmion-lattice phase from the Hall effect[17] and neutron diffraction measurements.[18] As shown in Fig. 1(a), the skyrmions and antiskyrmions in MnGe are anticipated to crystallize in a three-dimensional cubic structure.[18] The total spin chirality or the fictitious flux ($B_{\rm eff}$) on the skyrmion-antiskyrmion lattice is zero in zero magnetic field, but it can be activated by an external magnetic field to reach the maximum at an intermediate field strength in the magnetization process within the skyrmion crystal phase region [see Fig. 1(c)]. The simple-cubic skyrmion-lattice model well reproduces the overall H dependence of the Hall resistivity at 30 K.[18] The skyrmion-lattice constant λ has been estimated from the helical period determined by the neutron diffraction study:[17–19] λ changes from 6 to 3 nm with decreasing T and becomes almost constant ($\approx$3 nm) below 70 K [Fig. 1(b)].[17] The activated maximal $B_{\rm eff}$ should be proportional to the skyrmion density ($\propto 1/\lambda^3$), and the shortest λ value among known $B20$-type materials (10–100 nm for other materials) explains the largest topological Hall resistivity observed below 70 K in MnGe.[11–14,17] The magnitude of the topological Hall resistivity is nearly independent of T below 70 K, which is consistent with the constant value of λ in that T region [Fig. 1(b)].[17] The real-space fictitious flux at the lowest T is about -40 T,[17] which is estimated as the topological Hall resistivity divided by the normal Hall coefficient in analogy with the normal Hall effect.[16] The existence of the possible skyrmion-lattice phase and the emergence of the THE in such a wide T and H region of MnGe [Fig. 1(c)] motivate us to study topological thermal and thermoelectric transport properties related to the skyrmion lattice. In this paper, we investigate not only longitudinal but also transverse thermoelectric (Peltier) and thermal-conduction effects in the possible skyrmion-lattice phase of MnGe.

The thermal Hall and Nernst effects are thermal-conduction and thermoelectric counterparts of the electrical Hall effect, respectively. A heat current $\boldsymbol{j}^Q$ generates the temperature gradient $-\nabla T$ prescribed by $\boldsymbol{j}^Q = \boldsymbol{\kappa}(-\nabla T)$, where $\boldsymbol{\kappa}$ is a thermal conductivity tensor. An off-diagonal element κ_{xy} corresponds

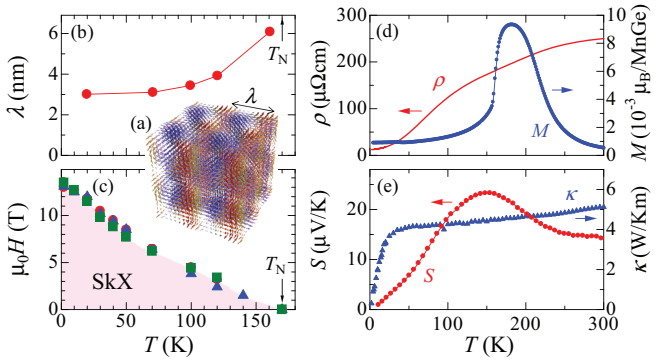

FIG. 1. (Color online) (a) A schematic illustration of a three-dimensional (simple cubic) skyrmion lattice possibly realized in MnGe. λ indicates the skyrmion-lattice constant. (b) Temperature (T) dependence of λ. λ changes from 6 to 3 nm with decreasing T.[17] The magnetic transition temperature (T_N) is 170 K in zero field. (c) Magnetic phase diagram determined from the H dependence of magnetization (M) (red circles), resistivity (ρ) (blue triangles), and Hall resistivity (ρ_H) (green squares).[17,18] The region denoted by "SkX" shows the possible skyrmion-lattice phase based on the assignment of Refs. 17 and 18 and the present study. (d) T dependence of resistivity (ρ) in zero field and magnetization (M) measured at 0.01 T. (e) T dependence of the Seebeck coefficient (S) and that of thermal conductivity (κ) in zero field.

to thermal Hall conductivity. The presence of the temperature gradient $-\boldsymbol{\nabla} T$ also induces the longitudinal and transverse open-circuit electric fields, i.e., $\boldsymbol{\sigma E} + \boldsymbol{\alpha}(-\boldsymbol{\nabla} T) = \mathbf{0}$. $\boldsymbol{\alpha}$ and $\boldsymbol{\sigma}$ are the thermoelectric (Peltier) and electrical conductivity tensors, respectively. The transverse Peltier conductivity α_{xy}, which is an intrinsic quantity of the Nernst effect, includes not only the Nernst signal (e_N) but also the contributions related with the Hall conductivity σ_{xy} and the thermal Hall conductivity κ_{xy}.[20] We thereby need the measurement of the thermal Hall effect to evaluate α_{xy} if $\nabla_y T \neq 0$. The conductivity tensors $\boldsymbol{\sigma}$, $\boldsymbol{\kappa}$, and $\boldsymbol{\alpha}$ are related with each other in the Boltzmann transport theory.[21] The ratio of $\boldsymbol{\kappa}$ to $\boldsymbol{\sigma}$ is $L_0 T$ ($L_0 = \pi^2 k_B^2 / 3e^2$: Lorenz number) regardless of materials if the scattering is elastic (the Wiedemann-Franz law).[21] A relation between $\boldsymbol{\alpha}$ and $\boldsymbol{\sigma}$ is known as the Mott relation: $\boldsymbol{\alpha} = eL_0 T(\partial \boldsymbol{\sigma}/\partial \varepsilon)_{\varepsilon=\mu}$, μ being the chemical potential.[21] These relations have been established recently for the anomalous and topological Hall effects associated with the momentum-space Berry phase,[22–27] while it has remained elusive for the THE caused by the real-space one.

II. EXPERIMENTS

We prepared high-density polycrystalline MnGe with a high-pressure (8 GPa) furnace.[17] The same specimen with a size of $3 \times 1 \times 0.1$ mm^3 was used for all the measurements of electrical Hall, thermal Hall, and Nernst effects. We performed the measurements in a superconducting magnet, in which the magnetic field (H) was applied along the z axis corresponding to the shortest dimension of the platelike sample. An electric current (in the Hall effect) or a temperature difference whose magnitude is a few percent of each measurement temperature (in Nernst and thermal Hall effects) was applied along the longest direction, which is defined as the x axis. The temperature difference was applied by Joule heating of a chip resistance (1 kΩ) and measured with Cernox thermometers (Lake shore Cryotronics Inc.) and type-E thermocouples. The Seebeck coefficient and the Nernst signal are defined as $S = E_x/|\nabla_x T|$ and $e_N = E_y/|\nabla_x T|$, respectively.[28,29] Longitudinal thermal conductivity and thermal Hall conductivity are obtained in the open-circuit condition of transverse heat current ($j_y^Q = 0$) as $\kappa = j_x^Q/|\nabla_x T|$ and $\kappa_H = \kappa \nabla_y T/\nabla_x T$, respectively.[30] From the measurements, longitudinal and transverse Peltier conductivities (α and α_H, respectively) were obtained using the relations that $\alpha = S\sigma$ and that $\alpha_H = \sigma[e_N + S\{(\sigma_H/\sigma) + (\kappa_H/\kappa)\}]$.[20] Here, σ and σ_H are the (longitudinal) electrical conductivity and Hall conductivity, respectively.

III. RESULTS AND DISCUSSIONS

Figure 1(d) shows the T dependence of resistivity $\rho(\approx \sigma^{-1})$ in zero field and magnetization M at $\mu_0 H = 0.01$ T. The resistivity exhibits a metallic behavior with the residual resistance ratio $\rho(300\text{ K})/\rho(2\text{ K}) \approx 19$. The T dependence and the magnitude of ρ and M are consistent with the results in the former report.[17] Shown in Fig. 1(e) are the T dependence of longitudinal thermal conductivity κ and that of the Seebeck coefficient S in zero field. κ decreases monotonically with decreasing T below 300 K. The magnitude of κ at 300 K (∼5 W/Km) is almost comparable with that of the same $B20$-type CoGe.[31] S in zero field has a positive sign in the whole T range below 300 K and shows a broad peak just below T_N. Such a peak structure just below T_N was reported in S of chromium ($T_N = 311$ K),[32] where a change in the band structure at the magnetic transition has been ascribed to an origin of the peak structure.[33] Also for MnGe, an electronic-structure change upon the magnetic transition may be responsible for the observed S anomaly.

We show the H dependence of the Nernst signal e_N in Fig. 2. Normal and anomalous Nernst signals are known to be proportional to H and M, respectively,[22] similarly to the case of Hall conductivity. As shown in Fig. 2, while the conventional (normal plus anomalous) terms of a positive sign are present below 160 K, the additional negative dip structure is clearly observed in the magnetization process in a wide T range between 30 and 140 K. Since the H region, in which the additional negative component has been observed, corresponds

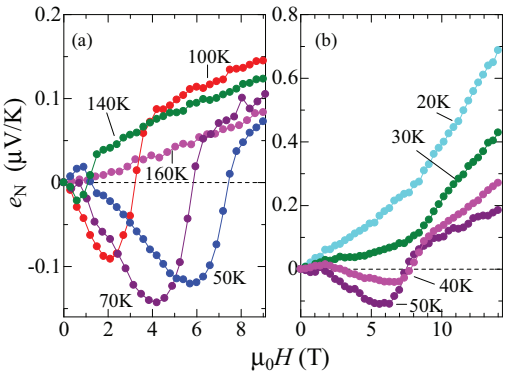

FIG. 2. (Color online) H dependence of the Nernst signal (e_N) at various temperatures below T_N.

to the possible skyrmion lattice phase [Fig. 1(c)],[17,18] this negative term in the Nernst effect should be related with the fictitious flux by the field-induced scalar spin chirality on the possible skyrmion lattice. It should be noted that the change in the band structure at the Fermi surface with H cannot explain the sign change in e_N, since the sign of e_N is the same in either electron or hole transport,[34] in contrast to the Hall effect or the Seebeck effect. With decreasing T down to 20 K, the topological term becomes obscured due to the large conventional ones [Fig. 2(b)]. According to the Mott relation, the Nernst signal is generally reduced linearly with T at low T's. The monotonic increase in conventional terms with decreasing T down to 20 K suggests a large change in the electronic structure near the Fermi level with H. In e_N, a kink structure, that is not discerned in the Hall resistivity,[17] is observed around 2 T at 30, 40, and 50 K. These kinks may correspond to the spin flop process arising from the competition between magnetic anisotropy and the Zeeman term, as suggested by M-H measurement.[17] Since the magnetic easy axis is ⟨100⟩,[17,18] the skyrmion-antiskyrmion lattice in the polycrystalline MnGe is randomly oriented with respect to the field direction in the low-field region, which results in the tiny topological term. As the magnetic field is increased above a threshold, the spin flop may occur so that the induced uniform magnetization of the skyrmion-antiskyrmion lattice aligns along the field direction, and accordingly the topological term becomes large.

In Figs. 3(a)–3(h), we compare the H dependence of the electrical Hall conductivity (σ_H) and the Nernst signal (e_N) at several T's below T_N. σ_H is composed of normal, anomalous, and topological Hall terms, i.e., $\sigma_H = \sigma_H^N + \sigma_H^A + \sigma_H^T$, where $\sigma_H^N = R_0\sigma^2(\mu_0 H)$ (normal Hall conductivity), $\sigma_H^A = R_s M$ (anomalous Hall conductivity), and σ_H^T (topological Hall conductivity).[17] As shown in Figs. 3(a)–3(d), the negative topological Hall term is clearly observed in the magnetization process below 50 K in addition to the anomalous Hall term proportional to M, whereas σ_H almost follows the change of M in the whole H region at 100 and 140 K [Figs. 3(c) and 3(d)]. Since the topological Hall conductivity σ_H^T is proportional to σ^2 [$\sigma_H^T = \sigma^2\rho_H^T \approx \sigma^2 R_0 B_{\rm eff}$ (ρ_H^T is the topological Hall resistivity)], σ_H^T becomes smaller in the higher-T region. In contrast, the topological term in e_N is clearly discerned in the high-T region up to 140 K [Figs. 3(f)–3(h)]; the T dependence of the topological term in e_N is distinct from that of σ_H^T, as shown in Figs. 3(e)–3(h). The magnitude of the topological term in e_N decreases slightly with increasing T above 50 K, but it remains more conspicuous than σ_H^T due to the relatively smaller conventional (normal and anomalous) terms in the Nernst effect.

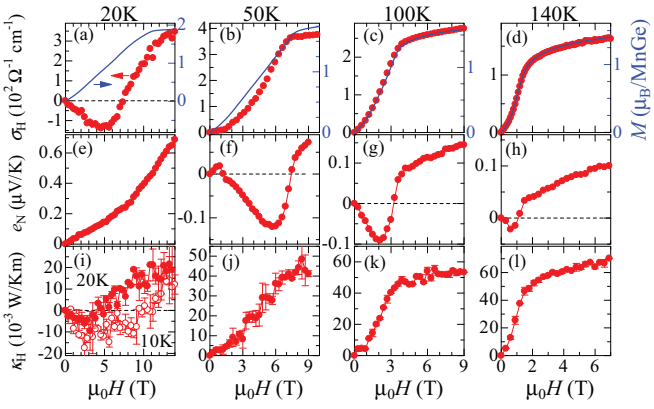

FIG. 3. (Color online) H dependence of (a)–(d) Hall conductivity (σ_H) [closed (red) circles] and magnetization (M) [solid (blue) lines], (e)–(h) Nernst signal (e_N), and (i)–(l) thermal Hall conductivity (κ_H) at several temperatures below T_N.

Figures 3(i)–3(l) show the H dependence of thermal Hall conductivity (κ_H). Also for κ_H, a negative dip corresponding to the topological Hall term is observed at 10 K [Fig. 3(i)]. With increasing T, however, the topological Hall term is suppressed more rapidly than in σ_H and can only be discerned up to 20 K. Above 50 K, the H dependence of κ_H is almost proportional to that of M (anomalous Hall term) [Figs. 3(j)–3(l)]. This rapid suppression of the topological Hall term in κ_H with T elevation is attributed to the influence of inelastic scattering (e.g., phonon scattering) on the topological Hall current. As demonstrated for longitudinal conductivity[21] and normal Hall conductivity,[25–27,30] the presence of inelastic scattering violates the Wiedemann-Franz law; thermal conductivity (κ or κ_H) becomes much lower than the value prescribed by the Wiedemann-Franz law ($L_0\sigma T$ or $L_0\sigma_H T$) due to the loss of heat current by inelastic phonon scattering.[21,25–27,30]

We obtain $\alpha_H = \sigma[e_N + S\{(\sigma_H/\sigma) + (\kappa_H/\kappa)\}]$ from the above data (σ, σ_H, S, e_N, κ, and κ_H) and show its H dependence in Figs. 4(a) and 4(b). From the Mott relations

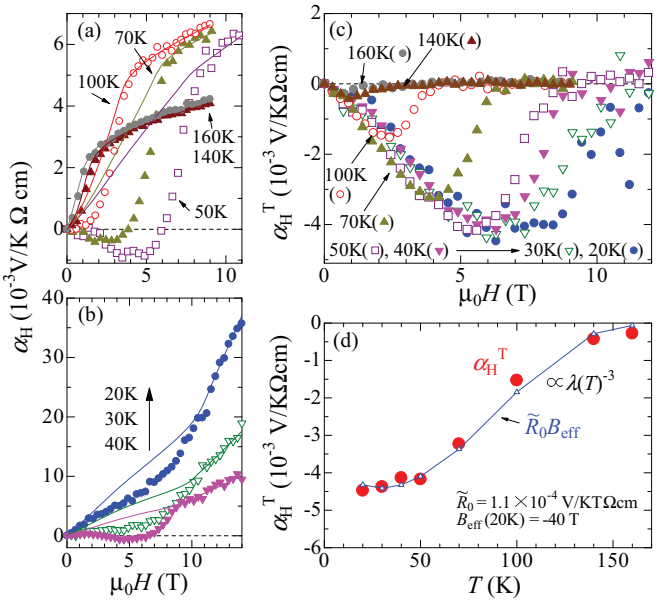

FIG. 4. (Color online) (a), (b) H dependence of α_H at various temperatures (T's) below T_N. Solid lines indicate the fitted curves using the conventional (normal and anomalous) terms except the topological term (see text). (c) H dependence of the estimated α_H^T below T_N. (d) The negative peak values of $\alpha_H^T(T)$ [$-|\alpha_H^T(T)|^{\rm max}$ [closed (red) circles] and $\tilde{R}_0 B_{\rm eff}(T)$ [open (green) triangles and solid (blue) line] in their H dependence at each T below 160 K. $|B_{\rm eff}|$ at 20 K is 40 T and decreases with increasing T through the change in the length scale of the spin texture (skyrmion-lattice constant, λ).[17] As a typical value of $\tilde{R}_0$, the value at 100 and 70 K ($\tilde{R}_0 = 1.1 \times 10^{-4}$ V/KT Ω cm) is used at all the T's.

[$\alpha = eL_0T(\partial\sigma/\partial\varepsilon)_{\varepsilon=\mu}$ and $\alpha_H = eL_0T(\partial\sigma_H/\partial\varepsilon)_{\varepsilon=\mu}$] as well as the empirical relation that $\sigma_H = R_0\sigma^2\mu_0 H + R_s M + \sigma_H^T$,[17] α_H is expressed as

$$\alpha_H = \left\{2\sigma\alpha R_0 + \frac{\pi^2}{3}\frac{k_B^2 T}{e}\sigma^2\left(\frac{\partial R_0}{\partial\varepsilon}\right)_{\varepsilon=\mu}\right\}\mu_0 H + \frac{\pi^2}{3}\frac{k_B^2 T}{e}\left(\frac{\partial R_s}{\partial\varepsilon}\right)_{\varepsilon=\mu} M + \alpha_H^T \quad (1)$$

$$\equiv \tilde{R}_0\mu_0 H + \tilde{R}_s M + \alpha_H^T. \quad (2)$$

The first term proportional to H and the second term proportional to M in (2) are assigned to the normal and anomalous Nernst terms, respectively. Since the topological term (α_H^T) does not exist above the saturation field of M, we fit α_H with $\alpha_H = \tilde{R}_0\mu_0 H + \tilde{R}_s M$ in the high-H region above the M saturation, as shown by solid lines in Figs. 4(a) and 4(b). Here, the fitting parameters are $(\partial R_0/\partial\varepsilon)_{\varepsilon=\mu}$ and $(\partial R_s/\partial\varepsilon)_{\varepsilon=\mu}$, which are assumed here to be constant with H, while the experimental values are used for all the other parameters in (1). The deviation in the course of the magnetization process between the observed α_H value and the fitted curve, i.e., $\alpha_H - \tilde{R}_0\mu_0 H - \tilde{R}_s M$, is assigned to the topological term α_H^T, as shown in Fig. 4(c). Although its magnitude is almost constant between 20 and 50 K, it begins to decrease monotonically with increasing T above 70 K.

Using $\sigma_H^T = \rho_H^T(\sigma)^2$, $\rho_H^T \approx R_0 B_{\rm eff}$, and Eq. (1), α_H^T is reduced to a simple form:

$$\alpha_H^T = \frac{\pi^2}{3}\frac{k_B^2 T}{e}\left(\frac{\partial\sigma_H^T}{\partial\varepsilon}\right)_{\varepsilon=\mu} \approx \tilde{R}_0 B_{\rm eff}. \quad (3)$$

Thus, α_H^T should be proportional to $B_{\rm eff}$ as obtained from the Hall effect measurement. In Fig. 4(d), we compare the negative peak values of α_H^T [Fig. 4(c)] and $\tilde{R}_0 B_{\rm eff}$ in their H dependence at each T. The T dependence of $B_{\rm eff}$ is estimated to be $B_{\rm eff} = -40$ T $[\lambda(T = 20\ {\rm K})/\lambda(T)]^3$ (Ref. 35) using the $\lambda(T)$ values [Fig. 1(b)] obtained from the neutron diffraction measurement.[17] As a typical value of $\tilde{R}_0$, we use the $\tilde{R}_0$ value at 100 and 70 K ($\tilde{R}_0 = 1.1 \times 10^{-4}$ V/KT Ω cm) in all the T region. As shown in Fig. 4(d), $\tilde{R}_0 B_{\rm eff}(T)$ well reproduces the T variation of α_H^T below 160 K. This validates the Mott relation for the topological Hall and Nernst effects on the topologically winding spin texture in MnGe. These topological transport phenomena share a common origin, namely the topological fictitious flux proportional to the density of the magnetic texture (maybe skyrmions). The fictitious flux, which was shown to be proportional not to λ^{-2} but to λ^{-3}, is consistent with the possible formation of the three-dimensional skyrmion lattice in MnGe.[18]

IV. CONCLUSIONS

We have performed a comprehensive study of Hall, thermal Hall, and Nernst effects in the noncoplanar spin-texture phase, which has been assigned to the three-dimensional skyrmion-lattice phase for MnGe. The topological term in thermal Hall conductivity rapidly decreases with increasing T due to the loss of topological heat current by inelastic scattering, while the topological term in the Nernst signal is clearly discerned and subsists even above 100 K. The experimentally obtained α_H^T is nearly proportional to the fictitious flux from the scalar spin chirality, in accord with the Mott relation. We have proved that the T dependence of α_H^T is proportional to λ^{-3} (λ being the length scale of the spin texture). This indicates that the skyrmions which have been anticipated to form the three-dimensional crystal structure are responsible for the topological transport phenomena in MnGe.

ACKNOWLEDGMENTS

This work was supported in part by Grants-in-Aid for Scientific Research (Grants No. 20340086, No. 24224009, and No. 25247058) and JSPJ Fellows, and by the Funding Program for World-Leading Innovative R&D on Science and Technology (FIRST program) on "Quantum Science on Strong Correlation."

*Present address: Institute for Materials Research, Tohoku University, Sendai 980-8577, Japan.

[1] T. H. R. Skyrme, Proc. R. Soc. London, Ser. A **260**, 127 (1961).
[2] S. Mühlbauer, B. Binz, F. Jonietz, C. Pfleiderer, A. Rosch, A. Neubauer, R. Georgii, and P. Böni, Science **323**, 915 (2009).
[3] C. Pfleiderer, T. Adams, A. Bauer, W. Biberacher, B. Binz, F. Birkelbach, P. Böni, C. Franz, R. Georgii, M. Janoschek, F. Jonietz, T. Keller, R. Ritz, S. Mühlbauer, W. Münzer, A. Neubauer, B. Pedersen, and A. Rosch, J. Phys.: Condens. Matter **22**, 164207 (2010).
[4] C. Pappas, E. Lelièvre-Berna, P. Falus, P. M. Bentley, E. Moskvin, S. Grigoriev, P. Fouquet, and B. Farago, Phys. Rev. Lett. **102**, 197202 (2009).
[5] W. Münzer, A. Neubauer, T. Adams, S. Mühlbauer, C. Franz, F. Jonietz, R. Georgii, P. Böni, B. Pedersen, M. Schmidt, A. Rosch, and C. Pfleiderer, Phys. Rev. B **81**, 041203(R) (2010).
[6] E. Moskvin, S. Grigoriev, V. Dyadkin, H. Eckerlebe, M. Baenitz, M. Schmidt, and H. Wilhelm, Phys. Rev. Lett. **110**, 077207 (2013).
[7] S. Seki, J. H. Kim, D. S. Inosov, R. Georgii, B. Keimer, S. Ishiwata, and Y. Tokura, Phys. Rev. B **85**, 220406(R) (2012).
[8] X. Z. Yu, Y. Onose, N. Kanazawa, J. H. Park, J. H. Han, Y. Matui, N. Nagaosa, and Y. Tokura, Nature (London) **465**, 901 (2010).
[9] X. Z. Yu, N. Kanazawa, Y. Onose, K. Kimoto, W. Z. Zhang, S. Ishiwata, Y. Matui, and Y. Tokura, Nat. Mater. **10**, 106 (2010).
[10] S. Seki, X. Z. Yu, S. Ishiwata, and Y. Tokura, Science **336**, 198 (2012).
[11] A. Neubauer, C. Pfleiderer, B. Binz, A. Rosch, R. Ritz, P. G. Niklowitz, and P. Böni, Phys. Rev. Lett. **102**, 186602 (2009).
[12] Y. Li, N. Kanazawa, X. Z. Yu, A. Tsukazaki, M. Kawasaki, M. Ichikawa, X. F. Jin, F. Kagawa, and Y. Tokura, Phys. Rev. Lett. **110**, 117202 (2013).
[13] M. Lee, W. Kang, Y. Onose, Y. Tokura, and N. P. Ong, Phys. Rev. Lett. **102**, 186601 (2009).

[14]S. X. Huang and C. L. Chien, Phys. Rev. Lett. **108**, 267201 (2012).
[15]T. Schulz, R. Ritz, A. Bauer, M. Halder, M. Wagner, C. Franz, C. Pfleiderer, K. Everschor, M. Garst, and A. Rosch, Nat. Phys. **8**, 301 (2012).
[16]M. Onoda, G. Tatara, and N. Nagaosa, J. Phys. Soc. Jpn. **73**, 2624 (2004).
[17]N. Kanazawa, Y. Onose, T. Arima, D. Okuyama, K. Ohoyama, S. Wakimoto, K. Kakurai, S. Ishiwata, and Y. Tokura, Phys. Rev. Lett. **106**, 156603 (2011).
[18]N. Kanazawa, J.-H. Kim, D. S. Inosov, J. S. White, N. Egetenmeyer, J. L. Gavilano, S. Ishiwata, Y. Onose, T. Arima, B. Keimer, and Y. Tokura, Phys. Rev. B **86**, 134425 (2012).
[19]O. L. Makarova, A. V. Tsvyashchenko, G. Andre, F. Porcher, L. N. Fomicheva, N. Rey, and I. Mirebeau, Phys. Rev. B **85**, 205205 (2012).
[20]Y. Onose, L. Li, C. Petrovic, and N. P. Ong, Europhys. Lett. **79**, 17006 (2007).
[21]N. W. Ashcroft and N. D. Mermin, *Solid State Physics* (Brooks Cole, Belmont, CA, 1976).
[22]W-L. Lee, S. Watauchi, V. L. Miller, R. J. Cava, and N. P. Ong, Phys. Rev. Lett. **93**, 226601 (2004).
[23]Y. Pu, D. Chiba, F. Matsukura, H. Ohno, and J. Shi, Phys. Rev. Lett. **101**, 117208 (2008).
[24]N. Hanasaki, K. Sano, Y. Onose, T. Ohtsuka, S. Iguchi, I. Kézsmárki, S. Miyasaka, S. Onoda, N. Nagaosa, and Y. Tokura, Phys. Rev. Lett. **100**, 106601 (2008).
[25]Y. Onose, Y. Shiomi, and Y. Tokura, Phys. Rev. Lett. **100**, 016601 (2008).
[26]Y. Shiomi, Y. Onose, and Y. Tokura, Phys. Rev. B **79**, 100404(R) (2009).
[27]Y. Shiomi, Y. Onose, and Y. Tokura, Phys. Rev. B **81**, 054414 (2010).
[28]Y. Wang, S. Ono, Y. Onose, G. Gu, Yoichi Ando, Y. Tokura, S. Uchida, and N. P. Ong, Science **299**, 86 (2003).
[29]Y. Wang, L. Li, and N. P. Ong, Phys. Rev. B **73**, 024510 (2006).
[30]Y. Zhang, N. P. Ong, Z. A. Xu, K. Krishana, R. Gagnon, and L. Taillefer, Phys. Rev. Lett. **84**, 2219 (2000).
[31]N. Kanazawa, Y. Onose, Y. Shiomi, S. Ishiwata, and Y. Tokura, Appl. Phys. Lett. **100**, 093902 (2012).
[32]J. P. Moore, R. K. Williams, and R. S. Graves, J. Appl. Phys. **48**, 610 (1977), and references therein.
[33]R. D. Barnard, *Thermoelectricity in Metals and Alloys* (Taylor & Francis, London, 1972).
[34]R. Bel, K. Behnia, and H. Berger, Phys. Rev. Lett. **91**, 066602 (2003).
[35]The value of B_{eff} at 20 K is obtained as $\rho_H^T/R_0 \approx -0.16\text{n}\Omega\,\text{cm}/4 \times 10^{-4}\text{cm}^3\,\text{C}^{-1} = -40$ T.